

Non-isothermal crystallization kinetics of polypropylene/MAP-POSS nanocomposites

Jungang Gao · Xinxin Cao · Chong Zhang · Wentao Hu

Received: 29 August 2011 / Revised: 12 October 2012 / Accepted: 2 January 2013 /
Published online: 9 January 2013
© Springer-Verlag Berlin Heidelberg 2013

Abstract Non-isothermal crystallization kinetics of polypropylene (PP)/methylacryloylpropyl polyhedral oligomeric silsesquioxanes (MAP-POSS) nanocomposites (PP/MAP-POSS) were investigated by DSC at various cooling rates. Jeziorny and Mo method were used to study the non-isothermal crystallization kinetics. The results show that the Jeziorny and Mo method are all successful in describing the non-isothermal crystallization kinetics of PP/MAP-POSS nanocomposites. The MAP-POSS can act a role of heterogeneous nucleation and increase the crystallization rate constant Z_c and decrease crystallization half time $t_{1/2}$, and the spherulitic crystal size decreases, the inter-spherulitic action or crosslinking structure each other appear at the appropriate content. The DSC peak temperature T_p increase about 5 °C, $t_{1/2}$ reduce 0.21 min at 6 % content of MAP-POSS and heating rate of 10 °C/min. The MAP-POSS can also increase the mechanical property of PP/MAP-POSS nanocomposites, the tensile strength and impact strength increase from 12.97 to 19.93 MPa and from 33.2 to 52.6 kJ/m², respectively, at 4 % content of MAP-POSS. But the spherulitic crystal becomes larger and boundaries become clearer again; the macrophase separation will occur and mechanical properties decrease when more and more MAP-POSS was added. The nanocomposite has the best mechanical property at 4 % content of MAP-POSS.

J. Gao (✉) · W. Hu
College of Chemistry and Environmental Science, Hebei University, Baoding 071002, China
e-mail: gaojg@hbu.edu.cn

X. Cao · C. Zhang
Institute of Materials Science and Engineering, Henan Polytechnic University,
Jiaozuo 454000, China

Keywords Polypropylene · Silsesquioxanes · Nanocomposite · Crystallization kinetics

Introduction

Polypropylene (PP), as important general plastics, has been widely used in many scopes such as packaging, transportation, machinery, electrical field, etc. But its application is limited by its easy aging and bad mechanical properties, and usually is modified by blend or copolymerization [1–3]. It is well known that the properties of PP significantly depend on its crystallization behavior. So it is important that investigate crystallization kinetics of PP and its composites [4, 5].

Organic–inorganic hybrid nanocomposite materials have been regarded as a new generation of high performance materials, since they combine the advantages of both inorganic materials (rigidity, high stability) and organic polymers (flexibility, low dielectric constant, ductility, and processability). Some researchers had reported that the polypropylene was modified by nanomaterials. Penco had reported the non-isothermal crystallization kinetics of polypropylene-layered double hydroxide composites [4]. Banerjee et al. [6] had reported the structural characterization of polypropylene/clay nanocomposite.

Polyhedral oligomeric silsesquioxane (POSS) has been shown to have great potential in the synthesis of organic/inorganic hybridized materials and thus has attracted much attention in recent years. The typical T_8 POSS monomers possess the structure of a cube-octameric framework with eight organic corner groups. The POSS is usually used as a modifier or reinforcer of polymeric materials. Compared with other modifiers it has a special cage structure and good compatibility with polymers. These organic functions make the POSS nanostructure compatible with many polymers or monomers. These enhancements have been shown to occur with a wide range of thermoplastic and thermoset systems [7, 8]. This makes them potentially useful for many engineering applications. Chen and Chiou [9] had reported the isothermal crystallization behavior and morphology of isotactic polypropylene blended with POSS. Fina et al. had reported the polypropylene/POSS nanocomposites which contained octamethyl, octaisobutyl, and octaisooctyl group [10]. They all find that the POSS can act as a nucleating agent of isotactic PP and increase the crystallization temperature by 2–3 °C.

In the methylacryloyloxy polyhedral oligomeric silsesquioxanes (MAP-POSS), the MAP contain unsaturated methacryl group, which can react with PP at higher temperature and modified the mechanical properties and crystalline morphology. In this paper, the effect of MAP-POSS on the non-isothermal crystallization kinetics of PP was investigated and discussed by Jeziorny method [11] and Mo method [12]. The mechanical properties of PP/MAP-POSS nanocomposite were determined. The results show that the Jeziorny and Mo method are all successful in describing the non-isothermal crystallization kinetics of PP/MAP-POSS nanocomposites. The MAP-POSS can act a role of heterogeneous nucleation and increase the mechanical properties, and has the best mechanical properties at the 4 % MAP-POSS content.

Experimental

Materials

The PP is isotactic polypropylene which is a commercial product and supplied by Yanshan Petrochemical Co. China; methylacryloylpropyl-trimethoxysilane (MAP-TMS) is chemical pure grade and supplied by Shenda Chem. Co. Beijing, China; Toluene, isopropyl alcohol (IPA) and tetramethylammonium hydroxide (TMAH) and benzoyl peroxide (BPO) are all analytically pure grades and supplied by the Tianjin Chemical Co., China.

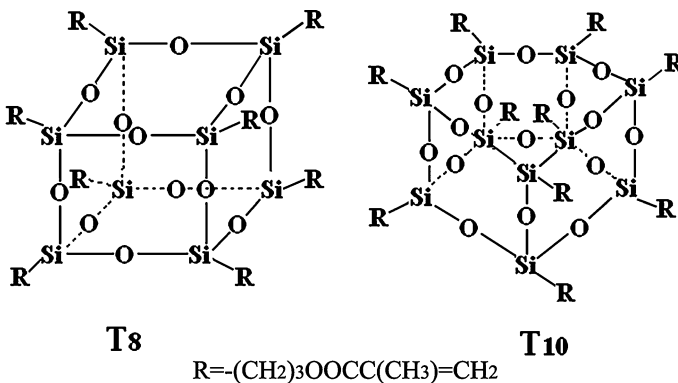
MAP-POSS was synthesized from MAPTMS by hydrolytic condensation and catalyzed with TMAH according literature [13] and [14], a transparent viscous liquid was obtained. The high performance liquid chromatography–mass spectrometer (LC/MSD, 1100 type, Agilent, USA) was used for the determination of the components and the detailed structure of MAP-POSS. The result shows that the product of eight silicon atoms cages T_8 was primary and contained a little T_{10} . The structure of MAP-POSS was showed as Scheme 1 [15].

Composites preparation

Composites containing 0, 1, 2, 4, 6, 8, 10, and 14 wt % MAP-POSS were prepared as follows: all components were first mixed in a mixer and then milled on a laboratory two-roll mill at 180 °C. The 5-mm thick plate was pressed at 170–180 °C, and cold pressed for 10 min at 5 MPa used to determine mechanical properties. In order to eliminate internal stress, the specimens were annealed in 90 °C. The corresponding specimens are marked as No.0, No.1, No.2, No.4, No.6, No.8, No.10 and No.14, respectively.

Non-isothermal crystallization measurement

A differential scanning calorimeter (DSC, Perkin–Elmer Diamond, USA) was used for calorimetric investigations of non-isothermal crystallization. DSC was calibrated



Scheme 1 Structures of MAP-POSS T_8 and T_{10}

with high purity indium. About 5 mg specimen was placed in a sealed aluminum sample pan and heated quickly from ambient temperature to 210 °C for 5 min to erase any previous thermal and mechanical history. After that the specimen was cooled to ambient temperature at constant cooling rates D of 5, 10, 15, 20 and 25 °C/min.

Characterization of phase morphology and mechanical properties

The phase behavior of the target compounds was characterized by polarizing optical microscopy (POM, BX51, Olympus Co. USA). According to ASTM D638 and D256, the tensile strength and impact strength were determined. Tensile strength test was performed using an electronic tensile tester (WSM-20kN, Changchun Tester Co, China). Tests were conducted at an extension rate of 10.0 mm/min at 25 °C and 50 % relative humidity. The notch impact test was carried out on an X CJ-40 impact tester (X CJ-40, Chengde Tester Co. China).

Results and discussion

Analyzing methods for the non-isothermal crystallization kinetics

Several models have been developed to describe the non-isothermal crystallization kinetics of polymers: such as the Jeziorny model are based on the Avrami equation [16], and read as:

$$1 - X(t) = \exp(-Z_t t^n), \quad (1)$$

where $X(t)$ is the relative crystallinity, Z_t is the crystallization rate constant, and n is the Avrami exponent. Here, the value of n depends on the nucleation mechanism and growth dimensions, and Z_t is a function of the nucleation and growth rate. $X(t)$ is a function of the crystallization time. For the non-isothermal crystallization process, the time t has the following relation with temperature T :

$$t = \frac{(T_0 - T)}{D}, \quad (2)$$

where T is the crystallization temperature at time t , and D is the cooling rate. The double logarithmic form of Eq. 1:

$$\log[-\ln(1 - X(t))] = n \log t + \log Z_t. \quad (3)$$

t can be converted from crystallization temperature, according to Eq. 2. After making the plot of $\log[-\ln(1 - X(t))]$ versus $\log t$, then the Avrami exponent n and the crystallization rate constant Z_t can be determined from the slope and intercept.

Considering the non-isothermal character of the process investigated, the crystallization rate of non-isothermal crystallization depends on the cooling rate; Jeziorny pointed out that the value of rate parameter Z_t should be corrected adequately [11]. Assuming a constant cooling rate or approximately constant D , the final form of kinetic rate constant at non-isothermal condition is given as below:

$$\log Z_c = \frac{\log(Z_t)}{D}. \quad (4)$$

Thus the crystallization half time, $t_{1/2}$, can be calculated from Eq. 5:

$$t_{1/2} = \left(\frac{\ln 2}{Z_c} \right)^{\frac{1}{n}}. \quad (5)$$

The crystallization kinetics of PP and PP/MAP-POSS was studied using Jeziorny method, and was also studied using Ozawa method [17] based on the Eq. 6.

$$1 - X(t) = \exp[-k(T)/D^m] \quad (6)$$

where $k(T)$ is the growth rate constant, $X(t)$ is the relative crystallinity at temperature T , D is the constant cooling rate, and m is the Ozawa exponent depends on the crystal growth and nucleation mechanism [17]. According to the Ozawa equation, From Eq. 6, we have:

$$\log[-\ln(1 - X(t))] = \log k(T) - m \log D. \quad (7)$$

In order to analyze the non-isothermal crystallization of specimens better, Mo [12] have proposed a new kinetic equation of non-isothermal crystallization by combining the Avrami equation and Ozawa equation:

$$\log Z_t + n \log t = \log k(T) - m \log D \quad (8)$$

or

$$\log D = \log F(T) - b \log t, \quad (9)$$

where the parameter $F(T) = [k(T)/Z_t]^{1/m}$ refers to the value of cooling rate, which has to be chosen at unit crystallization time when the measured system amounts to a certain degree of crystallinity, b is the ratio of the Avrami exponent n to the Ozawa exponent m .

Non-isothermal behavior of PP and PP/MAP-POSS

Figure 1 shows the DSC crystallization exothermal curves of PP, 2, 6, and 10 % MAP-POSS/PP samples at different heating rate (in order to simplify, the other DSC curves were not given in Fig. 1). As seen from Fig. 1, the crystallization peak temperature, T_p , decreases with increasing cooling rates (5, 10, 15, 20, and 25 °C/min). For example, the T_p of pure PP at a cooling rate of 5 °C/min is about 117.09 °C, while for a cooling rate of 20 °C/min it is 8.29 °C lower. A similar behavior was also observed for the PP/MAP-POSS composites. This could be that the crystallization process of polymeric molecular chain is a peristalsis process of chain segments, and it has a longer hysteresis time of molecular movement under the rapid cooling rate, so it has a lower T_p [12]. But under lower cooling rate, the molecular chains have sufficient time to peristalsis and nucleation, and the crystallization can proceed at a higher temperature. The plots of T_p variation at different cooling rate for the PP and PP/MAP-POSS composites are shown in Fig. 2. The T_p 's of PP and MAP-POSS/PP nanocomposites at different cooling rates are

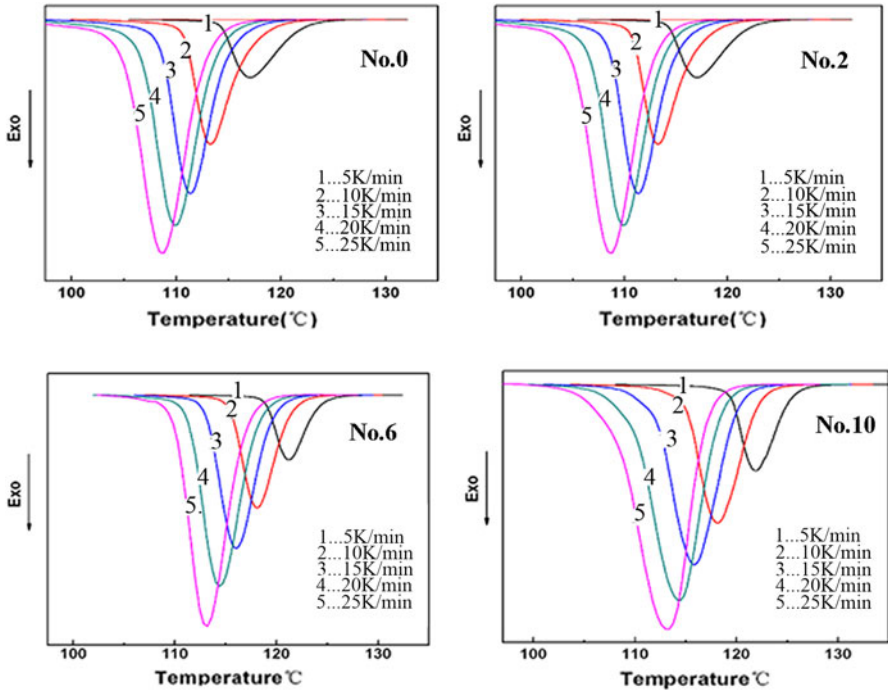
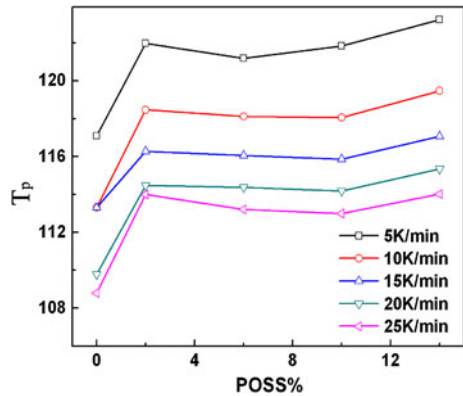


Fig. 1 DSC crystallization exothermal curves of PP and PP/MAP-POSS

Fig. 2 The variation of T_p at different cooling rate



shown in Table 1. As seen from Fig. 2 and Table 1, the T_p of nanocomposites at a given cooling rate is higher than that of pure PP, and similar results have also been found in some literatures [9, 10, 18]. This result clearly implies that the MAP-POSS plays the role of heterogeneous nucleation to promote the nucleation rate of PP in the crystallization process. However, with the increasing MAP-POSS content, the T_p has only a less change, this could be relate with the modality, dispersy, and nucleation mechanism of MAP-POSS in PP. When MAP-POSS is added, the

Table 1 The non-isothermal crystallization parameters of PP and PP/MAP-POSS at different cooling rates

Samples	D ($^{\circ}\text{C}/\text{min}$)	T_p	$t_{1/2}$ (min)	Avrami n	Z_c
No.0	5	117.09	1.82	3.65	0.60
	10	113.32	0.88	3.51	1.01
	15	111.3	0.64	3.47	1.08
	20	109.79	0.45	3.15	1.11
	25	108.80	0.40	3.54	1.12
No.2	5	121.97	1.40	3.16	0.75
	10	118.41	0.78	3.07	1.04
	15	116.28	0.49	3.10	1.13
	20	115.01	0.36	3.11	1.15
	25	114.00	0.34	3.13	1.13
No.6	5	121.19	1.28	3.32	0.79
	10	118.12	0.67	3.53	1.11
	15	116.07	0.46	3.50	1.18
	20	114.38	0.37	3.51	1.17
	25	113.21	0.32	3.18	1.14
No.10	5	121.85	1.45	3.60	0.71
	10	118.06	0.81	3.50	1.04
	15	115.86	0.53	3.45	1.13
	20	114.50	0.42	3.60	1.15
	25	113.00	0.34	3.19	1.13
No.14	5	123.23	1.33	3.49	0.76
	10	119.47	0.66	3.42	1.10
	15	117.07	0.48	3.53	1.16
	20	115.36	0.40	3.49	1.15
	25	114.02	0.37	3.45	1.16

individual regular MAP-POSS nanocrystal or small aggregate will attracts the PP molecular chains on the surface of MAP-POSS nanocrystal, and form a center of spherulite, acting as a sort of nucleating agent at small loading of MAP-POSS. So, the MAP-POSS can accelerate the crystalline growth and increasing T_p . But the solubility parameter of MAP-POSS with PP is different, thus the larger MAP-POSS aggregate will form with increasing content of MAP-POSS. This result will lead to microphase separation for MAP-POSS molecules with PP and form more and larger spherical crystal, so the No.6 has a little higher Z_t than No.4. But on the other hand, the small dispersed molecules state of MAP-POSS can also inhibit PP crystallization [9], so the T_p and $X(t)$ (at the same time) has a little decrease for more amount of MAP-POSS. Figure 3 shows the relationship of $X(t)$ with time for different contents of MAP-POSS. When more and more MAP-POSS was added, the macrophase separation will occur and macrocrystals will form and T_p also increases (as seen in Fig. 7), this phenomenon has also been proved by Chen and Chiou [9].

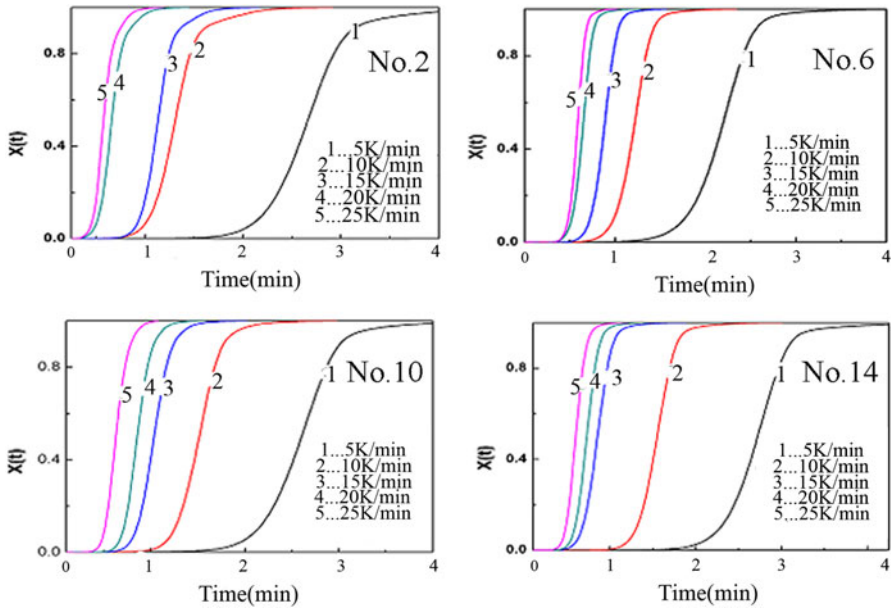


Fig. 3 Relative crystallinity $X(t)$ at various crystallization times

Non-isothermal crystallization kinetics based on Jeziorny method

Ozawa extended the Avrami equation to the non-isothermal case [17], which propounded that the non-isothermal crystallization process may be composed of infinitesimally isothermal crystallization steps. But some studied results had proved that the Ozawa analysis does not adequately describe the non-isothermal crystallization kinetics for some systems [18]. In these systems, the reason may be due to the secondary crystallization and inaccurate assumption or the disregard for the crystallization fold of the molecular chain which is a function of the crystallization temperature and time [19].

Figure 4 shows the $\log[-\ln(1 - X(t))]$ versus $\log t$ curves of PP/MAP-POSS nanocomposites. Table 1 summarizes values of the Avrami parameters n , Z_c and of $t_{1/2}$ for five specimens at different cooling rates. The crystallization constant, Z_c , increases with increasing cooling rates, while the crystallization half time, $t_{1/2}$, decreases. This is because both are the measurements of the overall crystallization rate, which will change with increasing the supercooling. After comparing MAP-POSS/PP and PP, it could be found that the $t_{1/2}$ of PP/MAP-POSS is less than that of PP, for a constant cooling rate, while Z_c increases, and similar results can also be found in some articles [20]. This proves that the crystallization behavior has been accelerated because of the presence of MAP-POSS. As seen from the Table 1, Z_c increases initially and then decreases, while $t_{1/2}$ has the opposite variation with increasing content of MAP-POSS. Specially, when the content of MAP-POSS is 6 %, the $t_{1/2}$ is the shortest and Z_c is the largest; this result indicate, when the content of MAP-POSS is 6 %, that the PP/MAP-POSS nanocomposite has the largest

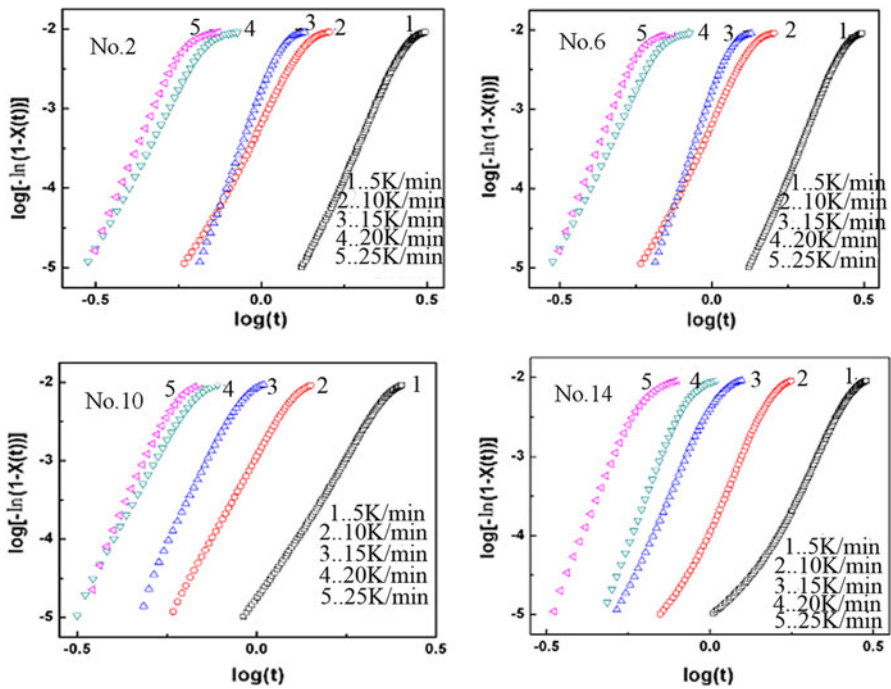


Fig. 4 Plots of $\log[-\ln(1 - X(t))]$ versus $\log t$ for PP/MAP-POSS nanocomposites on the Jeziorny method

overall crystallization rate. The regularity of Avrami crystallization exponent n is between 3 and 4 which do not change regularly and shows that the nucleation and crystallization growth of polypropylene is a complex way. The fractional value of n is to average contribution of simultaneous occurrence of various modes of nucleation and growth, that is, the heterogeneous nucleation of MAP-POSS and incomplete growth of spherulites occur simultaneously.

Non-isothermal crystallization kinetics described by the Mo method

A method developed by Mo was employed to the non-isothermal crystallization [12]. For the non-isothermal crystallization process, the physical variables relating to the process are relative crystallinity $X(t)$, cooling rate ϕ , and crystallization temperature T . At a given crystallinity $X(t)$, both the Ozawa and the Avrami equations can relate these variables as follows:

$$\log Z_t + n \log t = \log k(T) - m \log \phi. \tag{10}$$

And by rearrangement

$$\log \phi = \log F(T) - b \log t, \tag{11}$$

where $F(T) = [k(T)/Z_t]^{1/m}$ refers to the value of cooling rate, which must be chosen within unit of crystallization time when the measured system amounts to

certain crystallinity; and b is the ratio of the Avrami exponent n to Ozawa exponent m (n/m). According to Eq. (11), for a given relative crystallinity, the plot of $\log \phi$ versus $\log t$ will be obtained in a linear relation. The kinetic parameters $F(T)$ and b are determined from the intercept and the slope of the line, respectively. It is apparent that $F(T)$ has a definite physical and practical meaning. The plots of $\log \phi$ versus $\log t$ for PP and PP/MAP-POSS nanocomposites are given in Fig. 5. It is clear that there is a linear relationship between $\log \phi$ and $\log t$, and the linear correlation coefficients are in the range of 0.9913–0.9968. So this method has been proven to be applicable for these crystalline process. The values of $F(T)$ and b are listed in Table 2. As seen from Table 2, for each specimen, the values of b change slightly with the relative degree of the crystallinity. The value of $F(T)$ increases with increase in relative crystallinity for all samples studied, which shows that higher the relative crystallinity, the faster the cooling rate to achieve higher degree of crystallinity in unit time is. In general, at same relative degree of crystallinity, the values of $F(T)$ for PP/MAP-POSS nanocomposites are lower than of pure PP. This means that to reach the same degree of crystallinity, $X(t)$, the crystallization time of nanocomposites is shorter than pure PP. And when the content of MAP-POSS is 6 %, $F(T)$ is lowest, displaying that the overall crystallization rate is largest. These results are consistent with the above ones obtained from Jeziorny method, and indicate that MAP-POSS contributes to increase the overall crystallization rate of PP.

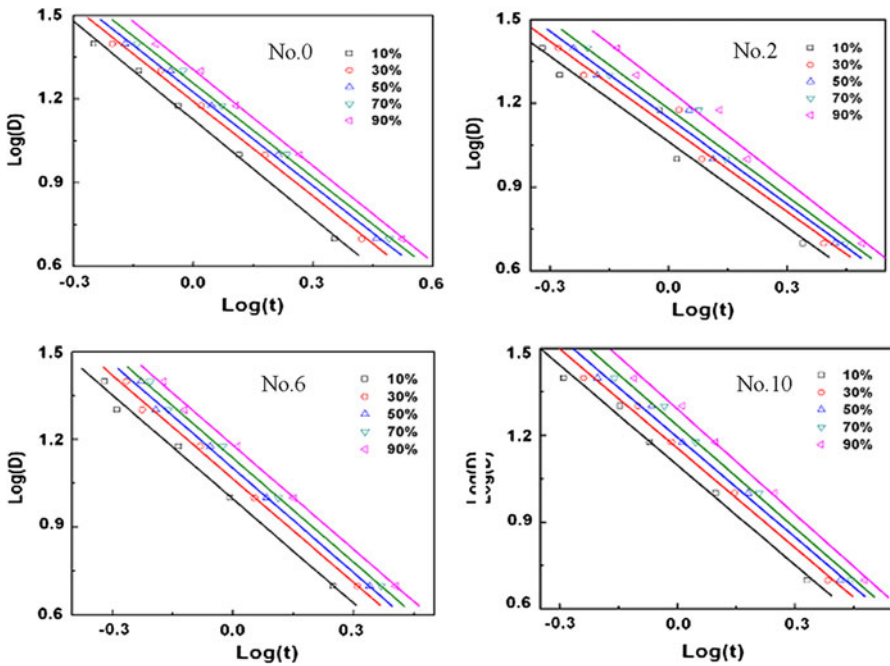


Fig. 5 The plots of $\log \phi$ versus $\log t$ for PP and PP/MAP-POSS

Table 2 Non-isothermal crystallization kinetic parameters of PP/MAP-POSS nanocomposites

Samples	$X(t)$	0.1	0.3	0.5	0.7	0.9
No.0	b	1.17	1.13	1.12	1.12	1.15
	$\log F(T)$	1.13	1.19	1.22	1.26	1.30
No.2	b	1.02	1.01	1.03	1.04	1.10
	$\log F(T)$	1.06	1.12	1.15	1.18	1.25
No.6	b	1.19	1.18	1.19	1.19	1.19
	$\log F(T)$	1.00	1.10	1.10	1.14	1.19
No.10	b	1.15	1.14	1.15	1.18	1.21
	$\log F(T)$	1.10	1.16	1.19	1.23	1.29
No.14	b	0.98	1.00	1.01	1.05	1.07
	$\log F(T)$	1.07	1.07	1.15	1.19	1.23

Dependence of mechanical properties on MAP-POSS content

The relationship of tensile strength and tensile modulus with MAP-POSS content are shown in Table 3, and the impact strength for different MAP-POSS content is shown in Fig. 6. As seen from Table 3 and Fig. 6, when MAP-POSS content is 4 %, the tensile strength, tensile modulus, and impact strength increase from 12.97, 310.2, and 33.2 kJ/m² of pure PP to 19.93, 366.9, and 52.6 kJ/m², respectively. Then they decrease with the increasing MAP-POSS content and have a best value at 4 % content. The reason is that MAP-POSS can increase the sliding resistance of intermolecules due to steric hindrance and production of part crosslink structure between PP and MAP-POSS, but plasticization of MAP-POSS in nanocomposite plays negative effect on mechanical properties when the MAP-POSS content is over than 4 %. Figure 7 shows the POM micrographs of PP and PP/MAP-POSS nanocomposites. As seen from Fig. 7, pure PP has a well-defined and large spherulite morphology, When the MAP-POSS content is 4 wt %, the spherulite size promptly decreases, and with less perfection, the right angle intersection disappears, the spherulite boundaries become more diffuse, and interspherulitic interaction or crosslinking structure increase. Although, the No.6 has the largest overall crystallization rate, the POM photograph of No.6 has a larger spherulites, smaller crosslinking spherulites, and clearer boundaries than No.4 (see Fig. 7), so it has lower mechanical properties than No.4. DSC results show that No.4 has the greatest degree of crystallinity, the melting enthalpy of crystallizing samples for No.0, No.4, No.6 and No.8 is 86.28, 107.79, 98.68, and 82.61 J/g, respectively. This is also one of the reasons for best mechanical properties of No.4. It is also shown that the MAP-

Table 3 Mechanical properties of PP/MAP-POSS nanocomposites

Samples:	No.0	No.1	No.2	No.4	No.6	No.8
Tensile strength (MPa)	12.97	15.15	19.13	19.93	17.98	12.52
Modulus (MPa)	310.2	313.4	315.7	366.9	391.2	390.4

Fig. 6 Relationship of impact strength and MAP-POSS content

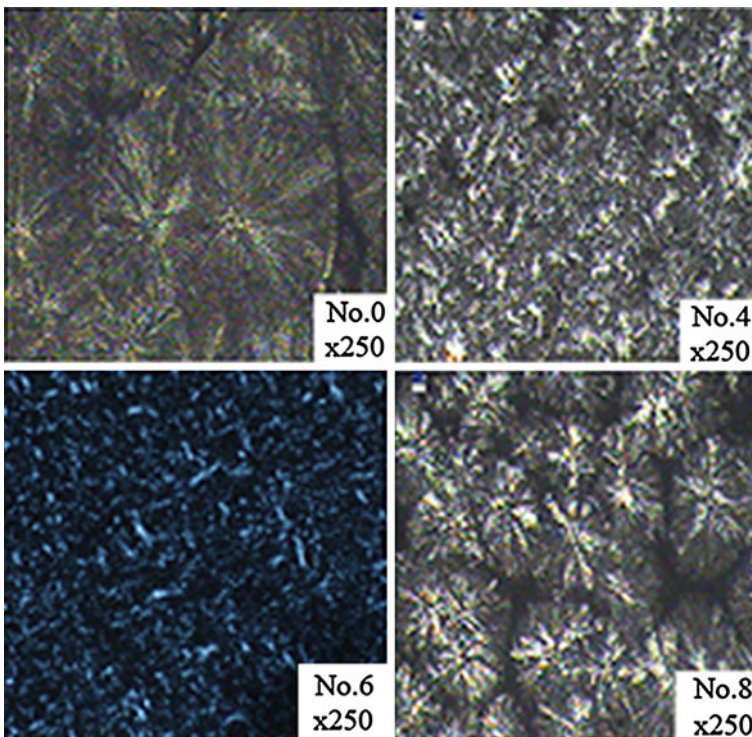
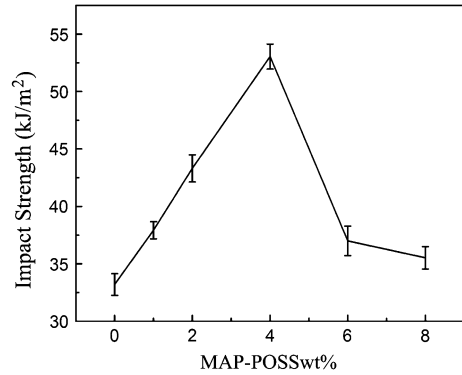


Fig. 7 The POM photographs of No.0, No.4, No.6 and No.8 nanocomposites

POSS has a role of heterogeneous nucleation and crosslinking reagent. Under this condition, the crystallizability of PP being disrupted by MAP-POSS, the PP molecular chains are more difficult to pack in an ordered manner than those of pure PP. In addition, the large number of nucleus centers causes more crystalline defects. The crosslink structure can increase tensile strength of materials and the partially methylacryloylpropyl group which does not react as a moving group can also increase impact strength of samples [15]. But crosslinking structure will decrease

with increasing MAP-POSS content again; when the MAP-POSS content is 8wt %, the spherulite morphology becomes larger and boundaries become more clear, so the mechanical properties decrease. This is because MAP-POSS has a larger congregation with one another than PP at higher content, and the macrophase separation will occur in the system [21].

Conclusions

The MAP-POSS can form nanocomposite with polypropylene. The Avrami equation modified by Jeziorny and Mo method can successfully describe the non-isothermal crystallization process of PP/MAP-POSS nanocomposites. The MAP-POSS in PP/MAP-POSS nanocomposites can act a role of heterogeneous nucleation and increase the crystallization rate constant Z_c and reduce the crystallization half time $t_{1/2}$ at the appropriate content. The spherulitic size decreases and the interspherulitic action or crosslinking structure increases, when the content of MAP-POSS is about 4 %. The MAP-POSS can also increase the mechanical property of PP/MAP-POSS nanocomposites, and has the best mechanical property at 4 % content of MAP-POSS, the tensile strength and impact strength increase from 12.97 to 19.93 MPa and from 33.2 to 52.6 kJ/m², respectively. But the spherulite crystal becomes larger and boundaries become clearer again; the macrophase separation will occur and mechanical properties decrease when more and more MAP-POSS was added.

Acknowledgments The authors gratefully acknowledge the financial support from the Nature Science Foundation (No. E2010000287) of Hebei Province, China.

References

1. Jipa S, Zaharescu T, Supaphol P (2010) Thermal stability of isotactic polypropylene modified with calcium carbonate nanoparticles. *Polym Bull* 64:787–790
2. Hieber CA (2002) Modeling/simulating the injection molding of isotactic polypropylene. *Polym Eng Sci* 42:1387–1409
3. Shi HC, Shi D, Yin LG, Luan SF, Yin JG et al (2010) Preparation of PP-g-PEG by using partial pre-irradiated polypropylene as initiator and its properties. *Polym Bull* 64:929–940
4. Penco M, Spagnoli G, Rahman MA et al (2011) Nonisothermal crystallization kinetics of polypropylene-layered double hydroxide composites: correlation with morphology. *Polym Compos* 32:986–993
5. Hu SF, Zhu XB, Hu W, Yan L, Cai C (2012) Crystallization behaviors and foaming properties of diatomite-filled polypropylene composites. *Polym Bull* 69. doi:10.1007/s00289-012-0849-0
6. Banerjee S, Joshi M, Ghosh AK (2010) A spectroscopic approach for structural characterization of polypropylene/clay nanocomposite. *Polym Compos* 31:2007–2016
7. Gao X, Wang W, Liu L (2010) A novel strategy to synthesize POSS/PS composite and study on its thermal properties. *Polym Bull* 64:15–25
8. Wang WP, Fei M, Jie XX, Wang P, Cao HM, Yu J (2010) Synthesis and characterization of star-shaped block copolymers with polyhedral oligomeric silsesquioxane (POSS) core via ATRP. *Polym Bull* 65:863–872
9. Chen JH, Chiou YD (2006) Crystallization behavior and morphological development of isotactic polypropylene blended with nanostructured polyhedral oligomeric silsesquioxane molecules. *J Polym Sci* 44:2122–2134

10. Fina A, Tabuani D, Frache A, Camino G (2005) Polypropylene–polyhedral oligomeric silsesquioxanes (POSS) nanocomposites. *Polymer* 46:7855–7866
11. Jeziorny A (1978) Parameters characterizing the kinetics of the non-isothermal crystallization of poly(ethyleneterephthalate) determined by DSC. *Polymr* 19:142–1148
12. Mo ZS (2008) A method for the non-isothermal crystallization kinetics of polymers. *Chin Polym Sinica* 7:656–660
13. Gao JG, Zhang YY, Zhang CY (2010) Nonisothermal co-polymerizing behavior and thermal properties of methylacryloylpropyl–POSS with styrene. *Polym Plast Technol Eng* 49(6):531–540
14. Kopesky E, McKinley G, Cohen R (2006) Toughened poly(methyl methacrylate) nanocomposites by incorporating polyhedral oligomeric silsesquioxanes. *Polymer* 47:299–309
15. Gao JG, Du YG, Dong CF (2010) Rheological behavior and mechanical properties of PVC/MAP-POSS nanocomposites. *Polym Compos* 31:1822–1827
16. Avrami M (1939) Kinetics of phase change I general theory. *J Chem Phys* 12:1103–1112
17. Ozawa TP (1971) Kinetics of the non-isothermal crystallization. *Polymer* 12:150–158
18. Kim SH, Ahn SH, Hirai T (2003) Crystallization kinetics and nucleation activity of silica nanoparticle-filled poly(ethylene 2,6-naphthalate). *Polymer* 44:5625–5634
19. Schmidt SC, Hillmyer MA (2001) Polylactide stereocomplex crystallites as nucleating agents for isotactic polylactide. *J Polym Sci* 39:300–313
20. Liu YH, Yang XT, Zhang W, Zheng SX (2006) Star-shaped poly(3-caprolactone) with polyhedral oligomeric silsesquioxane core. *Polymer* 47:6814–6825
21. Gao JG, Li SR, Kong DJ (2011) Reaction kinetics and physical properties of unsaturated polyester modified with methylacryloylpropyl–POSS. *J Polym Res* 18:621–626